

ISSN: (Print) (Online) Journal homepage: [www.tandfonline.com/journals/tbsd20](http://www.tandfonline.com/journals/tbsd20)


# Network pharmacology and molecular modelling study of *Enhydra fluctuans* for the prediction of the molecular mechanisms involved in the amelioration of nephrolithiasis

Bornika Chattaraj, Pukar Khanal, Arijit Nandi, Anwesha Das, Amit Sharma, Soumya Mitra & Yadu Nandan Dey


To cite this article: Bornika Chattaraj, Pukar Khanal, Arijit Nandi, Anwesha Das, Amit Sharma, Soumya Mitra & Yadu Nandan Dey (2023) Network pharmacology and molecular modelling study of *Enhydra fluctuans* for the prediction of the molecular mechanisms involved in the amelioration of nephrolithiasis, Journal of Biomolecular Structure and Dynamics, 41:24, 15400-15410, DOI: [10.1080/07391102.2023.2189476](https://doi.org/10.1080/07391102.2023.2189476)

To link to this article: <https://doi.org/10.1080/07391102.2023.2189476>

 View supplementary material [↗](#)

 Published online: 13 Mar 2023.

 Submit your article to this journal [↗](#)

 Article views: 263

 View related articles [↗](#)

 View Crossmark data [↗](#)

 Citing articles: 5 View citing articles [↗](#)



# Network pharmacology and molecular modelling study of *Enhydra fluctuans* for the prediction of the molecular mechanisms involved in the amelioration of nephrolithiasis

Bornika Chattaraj<sup>a\*</sup>, Pukar Khanal<sup>b\*</sup>, Arijit Nandi<sup>a</sup>, Anwesha Das<sup>c</sup>, Amit Sharma<sup>d</sup>, Soumya Mitra<sup>a</sup> and Yadu Nandan Dey<sup>a</sup>

<sup>a</sup>Department of Pharmacology, Dr. B. C. Roy College of Pharmacy and Allied Health Sciences, Durgapur, West Bengal, India; <sup>b</sup>Department of Pharmacology, Nitte Gulabi Shetty Memorial Institute of Pharmaceutical Sciences (NGSMIPS), NITTE University, Mangalore, India; <sup>c</sup>Department of Pharmacy, Indira Gandhi National Tribal University, Anuppur, India; <sup>d</sup>Department of Pharmaceutical Sciences and Technology, Birla Institute of Technology, Mesra, Ranchi, Jharkhand, India

Communicated by Ramaswamy H. Sarma

## ABSTRACT

In view of the ethno medicinal use of *Enhydra fluctuans* for the treatment of kidney stones; the present study aimed to elucidate the molecular mechanisms involved in the amelioration of nephrolithiasis through a network pharmacology approach. The phytoconstituents were queried in DIGEP-Pred to identify the regulated proteins. The modulated proteins were then enriched in the STRING to predict the protein-protein interactions and the probably regulated pathways were traced in the Kyoto Encyclopedia of Genes and Genomes. Further, the network was constructed using Cytoscape ver 3.5.1. Results showed that  $\beta$ -carotene was found to be regulating maximum targets i.e. 26. In addition, 63 proteins were triggered by the components in which the vitamin D receptor was targeted by the maximum phytoconstituents i.e. 16. The enrichment analysis identified the regulation of 67 pathways in which fluid shear stress and atherosclerosis-associated pathways (KEGG entry *hsa05418*) regulated ten genes. Further, protein kinase C- $\alpha$  was traced in 23 different pathways. In addition, the majority of the regulated genes were identified from the extracellular space via the modulation of 43 genes. Also, nuclear receptor activity had the maximum molecular function via the regulation of 7 genes. Likewise, the response to organic substance was predicted to trigger the top genes i.e. 43. In contrast, Stigmasterol, Baicalein-7-o-glucoside, and Kauran-16-ol were found to have a high affinity to bind with the VDR receptor confirmed by the molecular modelling and the dynamics. Hence, the study elucidated the probable molecular mechanisms of *E. fluctuans* in managing nephrolithiasis and identified the lead molecules, their targets, and possible pathways.

## ARTICLE HISTORY

Received 13 June 2022  
Accepted 28 February 2023

## KEYWORDS

*Enhydra fluctuans*; *in silico* study; kidney stones; nephrolithiasis; network pharmacology

## 1. Introduction


Urolithiasis is the occurrence of one or more calculi within the urinary tract (Ghelani et al., 2016). The current therapeutic antilithiatic agents include thiazide or alkali-citrate. Still, their uses are limited due to multiple adverse effects e.g. hypokalemia, hyponatremia, metabolic alkalosis, hypercalcemia, hyperglycemia, hyperuricemia, hyperlipidemia, and sulfonamide allergy (Pak, 1989). In addition, there is growing interest among the public in herbal medicine, particularly in the treatment of urolithiasis because of limited choice in pharmacotherapy. Previous studies revealed that the phytotherapeutic agents could be useful as either an alternative or an adjunctive therapy in the management of urolithiasis and many medicinal plants have been reported to be useful as antilithiatic agents (Sharma et al., 2016; Sikarwar et al., 2017). Though; traditional and folkloric medicines are highly efficacious, their

uses are limited due to a lack of knowledge and scientific evidence for their probable molecular mechanism due to the presence of multi constituents (Atanasov et al., 2021). The development of system biology tools and network pharmacology approach has helped to elucidate the mechanism of action of single and multi-components to understand and state the actions and interactions of the drug with multiple targets (Chandran et al., 2017; Khanal et al., 2019).

*Enhydra fluctuans* Lour. belongs to the family Asteraceae, which is majorly found in tropical and subtropical regions and found in Nepal, India, Bangladesh, Sri Lanka, Burma, and other southeast Asian countries. They are annual herbaceous, edible, and semi-aquatic plants whose leaves are bitter (Kuri et al., 2014), usually growing beside rivers, ponds, ditches, and other water bodies up to sea level 1,800 m (Rahman, 2019) at an ideal environmental temperature of 27°C to 35°C. In the ethno medicinal practices, the decoction of the

**CONTACT** Yadu Nandan Dey  [yadunandan.dey@bcrp.org](mailto:yadunandan.dey@bcrp.org); [yadunandan132@gmail.com](mailto:yadunandan132@gmail.com)  Department of Pharmacology, Dr. B. C. Roy College of Pharmacy and Allied Health Sciences, Durgapur, West Bengal 713206, India.

\*The authors contributed equally.

 Supplemental data for this article can be accessed online at <https://doi.org/10.1080/07391102.2023.2189476>.

whole plant of *E. fluctuans* is consumed by various tribes of the Northeast region of India and Bangladesh to treat kidney stones and urinary problems (Swapana et al., 2011). *In vitro* studies also revealed that *E. fluctuans* has an inhibitory role in calcium oxalate crystallization (Chattaraj et al., 2022). Because of the ethno medicinal use of *E. fluctuans* for the treatment of kidney stones; the present study aimed to elucidate the molecular mechanisms involved in ameliorating nephrolithiasis through the network pharmacology approach.

## 2. Materials and methods

### 2.1. Source of phytoconstituents

The reported phytoconstituents were obtained from published literature (Barua et al., 2021), and their simplified molecular input line entry system (SMILES) were obtained from PubChem (<https://pubchem.ncbi.nlm.nih.gov/>) open-source database.

### 2.2. Identification of targets

The SMILES of all compounds were queried in DIGEP-Pred (<http://www.way2drug.com/ge/>) to identify the probably regulated proteins at pharmacological activity >0.5 (Lagunin et al., 2013). DIGEP-Pred web service provides the list of upregulated and downregulated targets of ligands (small molecules).

### 2.3. Enrichment analysis and network construction

The identified proteins were then enriched in the STRING (<https://string-db.org/>) (Szklarczyk et al., 2019) to predict the protein-protein interactions, and the probably regulated pathways were traced concerning the KEGG (<https://www.genome.jp/kegg/pathway.html>) (Kanehisa et al., 2016). In addition, three GO terms namely cellular components, molecular function, and biological process were also predicted. Further, the network between the phytoconstituents, proteins, and pathways was constructed using Cytoscape (<https://cytoscape.org/>) ver 3.5.1 (Shannon et al., 2003) which was later interpreted via edge count score.

## 2.4. Molecular docking

### 2.4.1. Protein preparation

The VDR receptor coordinates were retrieved from the RCSB protein data bank (PDB ID 1IE8). The protein structure was prepared using the Protein Preparation Wizard (PPW) and its quality was examined and adjusted by adding the missing residues by using the Prime module of Schrödinger suite 2017-2 (Sastry et al., 2013; Protein preparation wizard, 2017). The water molecules were removed from the crystallized protein structure. The network of H-bond was optimized and the overlapped hydrogen atoms were fixed under the refine tab of PPW. The pH was set to 7.0 and the protein was minimized by applying the OPLS3 force field by performing restrained minimization until the average root mean square deviation (RMSD) of the non-hydrogen atoms converged to 0.30 Å.

### 2.4.2. Ligand preparation

The chemical structure of the best binding energy-containing VDR regulating phytoconstituent, i.e, stigmasterol was retrieved in structure-data file (.sdf) format from the PubChem database. The molecule was imported into the Maestro interface of Schrödinger. The molecules were energy minimized and their 3D conformers were generated using the OPLS3 force field in the LigPrep module of Schrödinger software (Schrödinger Release 2017-2: LigPrep, 2017). The enumeration of ionization states was done for stigmasterol at a pH of 7.4 using Epik.

### 2.4.3. Ligand-protein docking

Molecular docking studies were performed by using the GLIDE (Grid-based Ligand Docking with Energetics) docking module of Schrödinger suite 2017-2, wherein, the prepared ligands were docked into the generated receptor grid using Glide SP docking precision (Friesner et al., 2004; Schrödinger Release 2017-2: Glide, 2017). It uses a grid-based ligand docking method with energy that searches for favorable interactions between a ligand and a receptor molecule like protein. The selected Van der Waals scaling factor and the partial charge cut-off were 0.80 and 0.15, respectively, for ligand atoms. The interactions of each complex were analyzed and the 3D poses demonstrating the molecular recognition interactions were obtained using the Schrödinger suite 2017-2. To validate the docking protocol, the bound ligand (KH1060) was extracted from the prepared protein structure and was redocked, after which the RMSD was determined.

## 2.5. Molecular dynamics

The molecular dynamics step was carried out to validate the molecular docking step, by checking the conformational stability of Stigmasterol-1IE8 docked complex. The Desmond module of Schrödinger software was utilized for performing a molecular dynamic simulation of docked complexes of analogs stigmasterol. Using a system builder panel, the orthorhombic box was prepared. The docked ligand-protein complex was solvated using the SPC water model. The MD simulation was performed using an NPT ensemble at a temperature of 310K and an atmospheric pressure of 1.013 bar for 100 ns. The results of molecular dynamics simulation were analyzed using simulation interaction diagram features of the Desmond software (Desmond, 2017, Nandi et al., 2023; Auti et al., 2022).

## 2.6. In silico physico-chemical and ADME/T studies

The drug likeliness of the best three compounds was evaluated in terms of the physicochemical parameters and key pharmacokinetic properties through and Swiss ADME web-server (Daina et al., 2017). The ADME/T and physicochemical analysis of phytoconstituents is discussed in the "Results" section below.

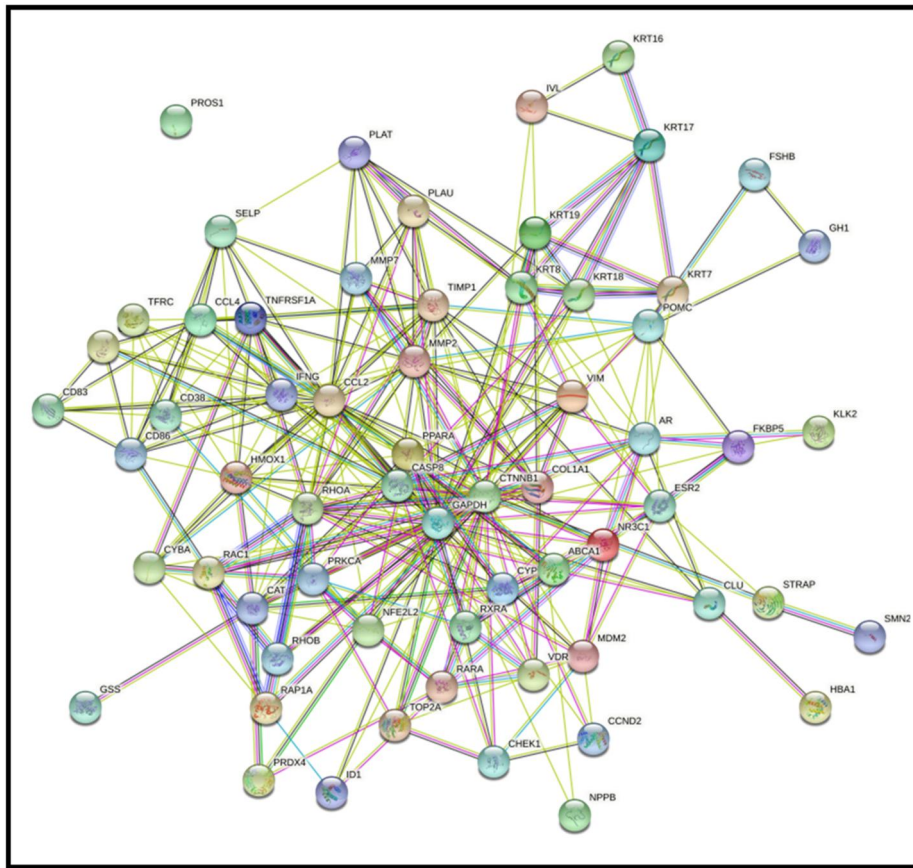


**Figure 1.** Protein-protein interaction of the regulated targets by the phytoconstituents from *Enhydra fluctuans* Lour. Colored nodes: query proteins and first shell of interactors, white nodes: second shell of interactors, node content; empty nodes: proteins of unknown 3D structure, filled nodes: some 3D structure are known or predicted.

### 3. Results

#### 3.1. Network pharmacology

A total of 25 phytoconstituents were traced in which beta-Carotene was identified to target the maximum number of proteins i.e. 26 (Table S1).

In addition, 63 different proteins were determined to be regulated by the phytoconstituents in which VDR was targeted by the maximum phytoconstituents i.e. 16; (Table S2).

Also, enrichment analysis of protein-protein interaction (Figure 1) identified the regulation of 67 pathways. In KEGG analysis, the majority of the regulated proteins by the phytoconstituents were also involved in the Fluid shear stress and atherosclerosis. Herein, a total of 10 genes were modulated i.e. *TNFRSF1A*, *HMOX1*, *MMP2*, *PLAT*, *CCL2*, *IFNG*, *CYBA*, *CTNNB1*, *NFE2L2*, and *RHOA* at 1.38 strength and 1.04E-08 false discovery rate.

In addition, multiple pathways like hypoxia-inducible factor 1 (HIF-1), p53, Wnt, Nuclear factor kappa B (NF-κB), Toll-like receptor, Rap1, cyclic Adenosine Monophosphate (cAMP), phosphatidylinositol 3-kinase and protein kinase B (PI3K-Akt), Transforming growth factor beta (TGF-β), interleukin (IL-17), and tumor necrosis factor (TNF) signalling pathway, and cytokine-cytokine receptor interaction were also traced via the combined action of phytoconstituents. Further, protein kinase C alpha (PRKCA) was predicted to be majorly traced in multiple pathways within the regulated pathways i.e. 23; (Table S3).

In addition, the majority of the regulated genes were regulated from the extracellular space via the modulation of 43 genes namely *TNFRSF1A*, *HMOX1*, *GSS*, *TIMP1*, *MMP2*, *PLAT*, *CCL2*, *COL1A1*, *CD38*, *IFNG*, *GAPDH*, *CAT*, *MMP7*, *SELP*, *RHOB*, *KRT16*, *CD14*, *GH1*, *KLK2*, *CLU*, *HBA1*, *KRT7*, *CD86*, *CTNNB1*, *RAC1*, *TFRC*, *KRT19*, *IVL*, *RAP1A*, *PLAU*, *NPPB*, *PRDX4*, *KRT18*, *PROS1*, *POMC*, *CHEK1*, *RHOA*, *PRKCA*, *FSHB*, *FKBP5*, *VIM*, *KRT8*, and *CCL4* against 3195 background genes (0.62 strength and 1.81E-16 false discovery rate); (Table S4).

Also, nuclear receptor activity had the maximum molecular function via the regulation of 7 genes namely *NR3C1*, *RARA*, *ESR2*, *AR*, *PPARA*, *RXRA*, and *VDR* against 48 background genes (1.66 strength and 2.34E-06 false discovery rate); (Table S5).

Likewise, the response to organic substances regulated the maximum genes i.e. 43; *TNFRSF1A*, *HMOX1*, *GSS*, *TIMP1*, *MMP2*, *CCL2*, *COL1A1*, *CD38*, *IFNG*, *GAPDH*, *NR3C1*, *CAT*, *RARA*, *MDM2*, *CYBA*, *SELP*, *CD14*, *GH1*, *CLU*, *CD86*, *ESR2*, *CTNNB1*, *CASP8*, *TFRC*, *KRT19*, *RAP1A*, *AR*, *ABCA1*, *ID1*, *CD83*, *CYP11A1*, *KRT18*, *NFE2L2*, *POMC*, *PPARA*, *RHOA*, *PRKCA*, *FSHB*, *RXRA*, *VIM*, *VDR*, *KRT8*, and *CCL4* against 3011 background genes (0.65 strength and 1.28E-16 false discovery rate); supplementary file, Table S3. Likewise, the interaction of the phytoconstituents with respective proteins and proteins concerned with their pathways are presented in Figures 2 and 3, respectively.

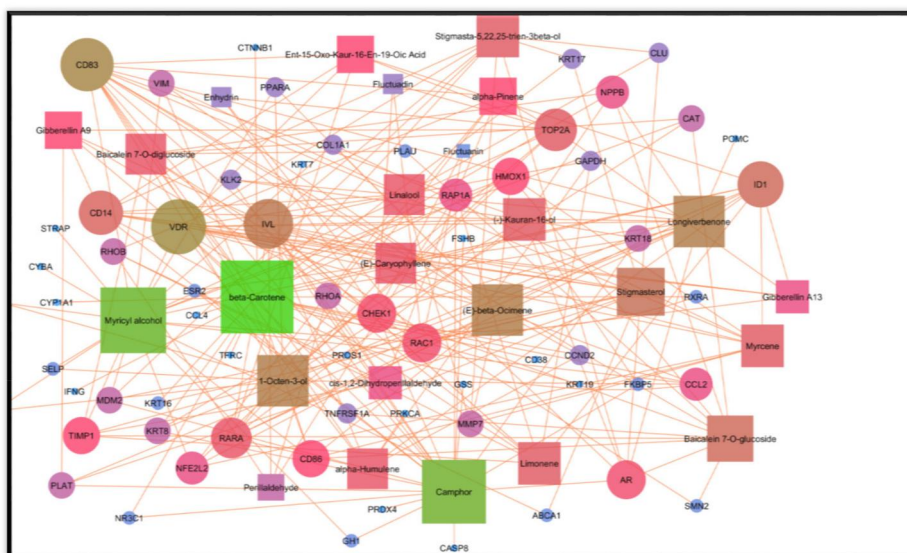


**Figure 2.** Interaction of the phytoconstituents from *Enhydra fluctuans* Lour and their targets. In the above figure square represents the phytoconstituents and circle presents the targets.

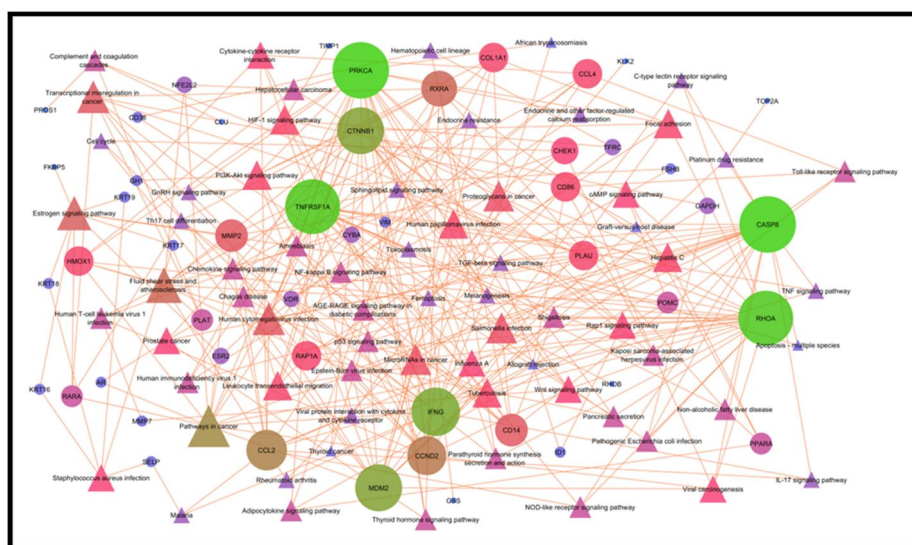


**Figure 3.** Interaction of phytoconstituents-regulated proteins with their respective pathways. Circle represents the target and triangle represents the signalling pathways.

### 3.2. Ligand-protein docking

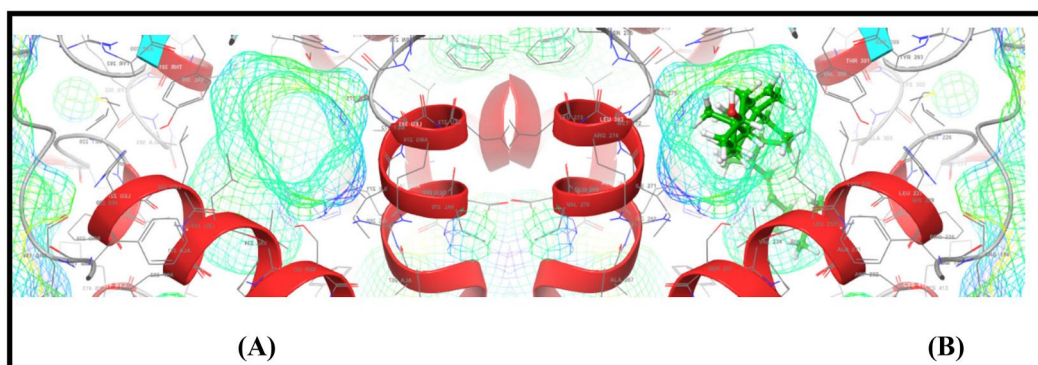
This molecular docking simulation study suggested that the top ranked conformations of phytoconstituents were well lodged at the active binding site of *VDR* receptor (Figure 4).

Table 1 showed the results of docking along with the major interactions for stigmasterol and baicalein-7-o-glucoside with *VDR* receptor with Glide scores  $-10.538$  and  $-9.964$  kcal/mol which is higher than that of the internal control, KH1060 ( $-9.790$  kcal/mol). The phytoconstituent kauran-16-ol has the Glide scores of  $-9.688$  kcal/mol which is also comparable with the internal control. The results of docking along with the major interactions of other compounds were mentioned in Table S6.

Figure 5 showed the binding pose and detailed protein interaction of stigmasterol, baicalein-7-o-glucoside, and kauran-16-ol

within the active site of *VDR* receptor. Several hydrophobic and polar interactions observed between the stigmasterol, baicalein-7-o-glucoside, kauran-16-ol and the active site residues, stabilize the binding of this phytoconstituents in the binding site of *VDR* receptor. There is only one H-bond was observed between the stigmasterol and the *VDR* receptor.

Superimposition of internal control, KH1060 and best docked pose of stigmasterol, baicalein-7-o-glucoside, and kauran-16-ol at the active pocket of *VDR* is depicted in Figure 6, which reveals that stigmasterol, baicalein-7-o-glucoside, kauran-16-ol, and KH1060 share a common binding pattern. Hydrophobic alkyl chain of the co-crystallized ligand and the three phytoconstituents are overlapping. The docking analysis, revealed good hydrophobic contacts of and the three phytoconstituents with the *VDR*, which may be responsible for the strong binding affinity. Thus, the molecular docking results, allow us to believe that



**Figure 4.** The active site of the VDR receptor (A) and the stigmasterol is docked into the active site (B).

**Table 1.** Molecular docking results of the phytoconstituents and KH1060, showing various types of interactions.

Compounds	Binding energies (Kcal/mol)	H-bond forming amino acid residues	Polar contacts forming amino acid residues	Hydrophobic interaction forming amino acid residues
Stigmasterol	-10.538	Ser 278	Ser 237, Ser 275, Ser 278, His 305, His 397	Tyr 143, Phe 150, Leu 227, Leu 230, Ala 231, Leu 233, Val 234, Ile 268, Ile 271, Met 272, Trp 286, Cys 288, Tyr 295, Val 300, Ala 303, Leu 309, Leu 313, Tyr 401, Leu 404, Leu 414, Val 418, Phe 422
Baicalein-7-o-glucoside	-9.964	Ser 278	Ser 237, Ser 275, Ser 278, His 305, Gln 317, His 397	Tyr 143, Tyr 147, Phe 150, Leu 227, Leu 230, Ala 231, Leu 233, Val 234, Ile 268, Ile 271, Met 272, Trp 286, Cys 288, Tyr 295, Val 300, Ala 303, Leu 313, Leu 404, Leu 414
Kauran-16-ol	-9.688	Ser 237	Ser 237, Ser 275, Ser 278	Tyr 143, Tyr 147, Phe 150, Leu 230, Leu 233, Val 234, Tyr 236, Ile 271, Trp 286, Cys 288, Tyr 295, Val 300, Leu 313
KH1060 (Co-crystal)	-9.790	Ser 237	Ser 237, Ser 275, Ser 278, His 305, His 397	Tyr 143, Tyr 147, Phe 150, Leu 227, Leu 230, Ala 231, Leu 233, Val 234, Tyr 236, Ile 268, Ile 271, Met 272, Trp 286, Cys 288, Tyr 295, Val 300, Ala 303, Leu 313, Tyr 401, Leu 404, Leu 414, Val 418, Phe 422

stigmasterol, Baicalein-7-o-glucoside, and Kauran-16-ol have potential to inhibit VDR receptor through an action on binding site.

### 3.3. Molecular dynamics

**Molecular dynamics:** Molecular dynamics simulations of protein-ligand complexes is considered as the most mature technique in the domain of computer-aided drug design (CADD) in terms of the evaluation of the macromolecular structure to-function correlation. In this current study, the impartial molecular dynamics study was performed to demystify the stability of the docked pose of three best binding energy-containing phytoconstituents [Stigmasterol, baicalein 7-O-glucoside, and (-)-kauran-16-ol] with vitamin D receptor (VDR). With the generation of 100 ns MD simulations the root mean square deviation (RMSD), the root mean square fluctuation (RMSF), protein-ligand contacts were generated and carefully analysed their significance in the solidity of the protein-ligand complexes (Figure 7).

**Stability analysis:** For the evaluation of dynamic stability of the protein-ligand complexes the RMSD was selected as a criterion. We decided to analyse the best docking pose of the top three dock scoring phytoconstituents against VDR receptor in terms of binding interactions. For this, the

queried protein frame was aligned against the reference frame to check the median replacement of atoms, in this cases  $\text{C}\alpha$ . In the case of small, globular proteins the replacement of  $< 3 \text{ \AA}$  in RMSD evolution (left Y-axis) is acceptable. Ligand RMSD clearly stipulates the stability of the ligand concerning the protein and its binding site. Here the 'Lig fit Prot' revealed that the RMSD of a ligand when the protein-ligand complex was aligned first time on the mainstay of the reference protein and the RMSD of the heavy atoms were estimated. Nevertheless, the greater replacement stipulate higher conformational change during the simulation. However, the RMSD of stigmasterol-VDR complex for the first few nanoseconds is also more than  $1.5 \text{ \AA}$  after some time it goes up to  $3.0 \text{ \AA}$  and afterward goes up to  $4.8 \text{ \AA}$  and stabilizes there. From the stability analysis of baicalein 7-O-glucoside with VDR receptor, it was found that the RMSD of baicalein 7-O-glucoside-VDR complex for the first few nanoseconds is  $1.2 \text{ \AA}$  after some time it goes up to  $2.4 \text{ \AA}$  and afterward goes up to  $2.8 \text{ \AA}$  and stabilizes there. Whereas from the stability analysis of (-)-kauran-16-ol with VDR receptor, it was found that the RMSD of (-)-kauran-16-ol-VDR complex for the first few nanoseconds is  $1.2 \text{ \AA}$  after some time it goes up to  $2.4 \text{ \AA}$  and afterward goes up to  $2.8 \text{ \AA}$  and stabilizes there.

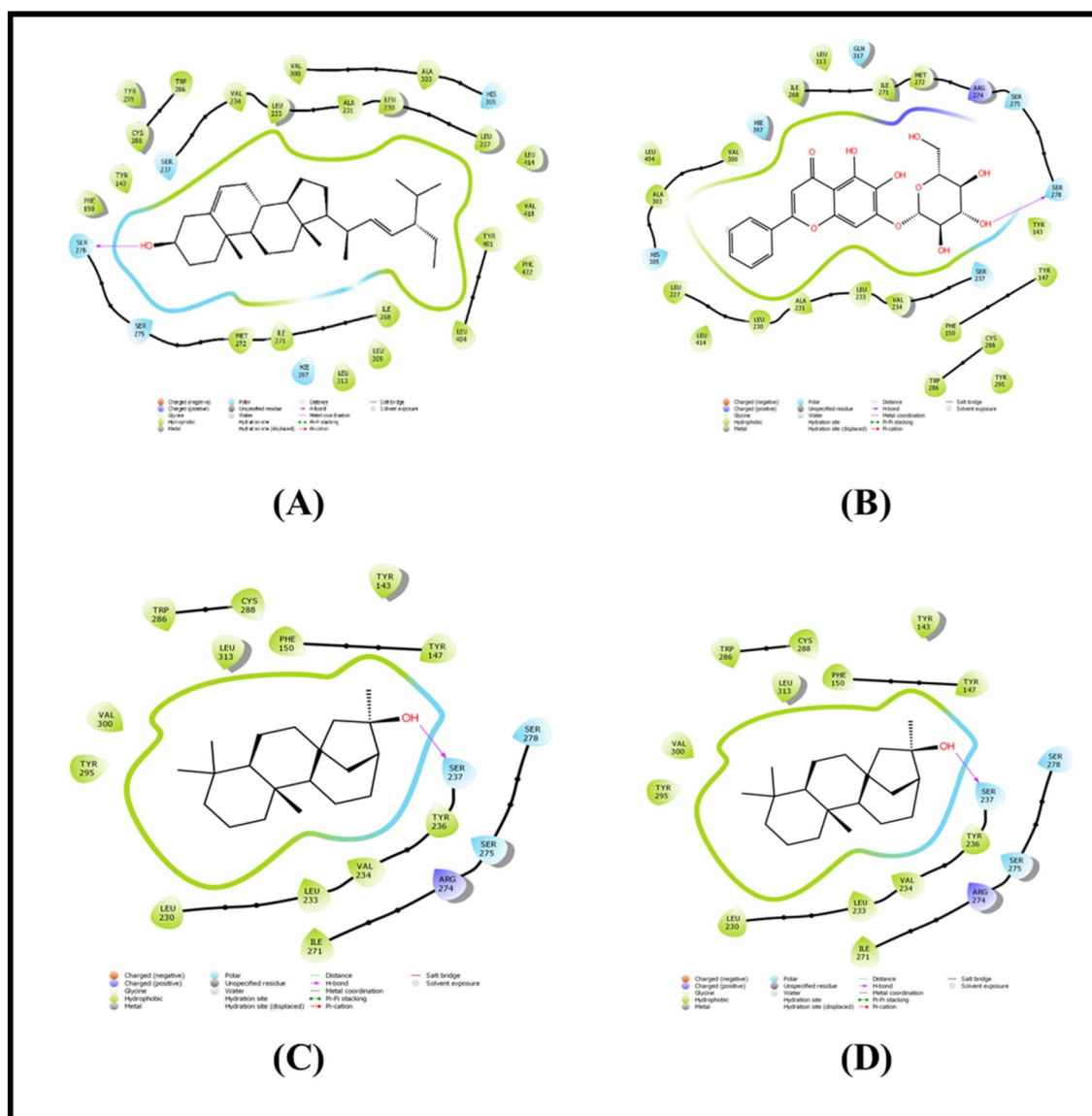


Figure 5. 2D interaction diagram of stigmaterol (A), baicalein-7-o-glucoside (B), kauran-16-ol, (C) and internal control KH1060 (D) at the active site of the VDR (PDB ID: 1IE8).

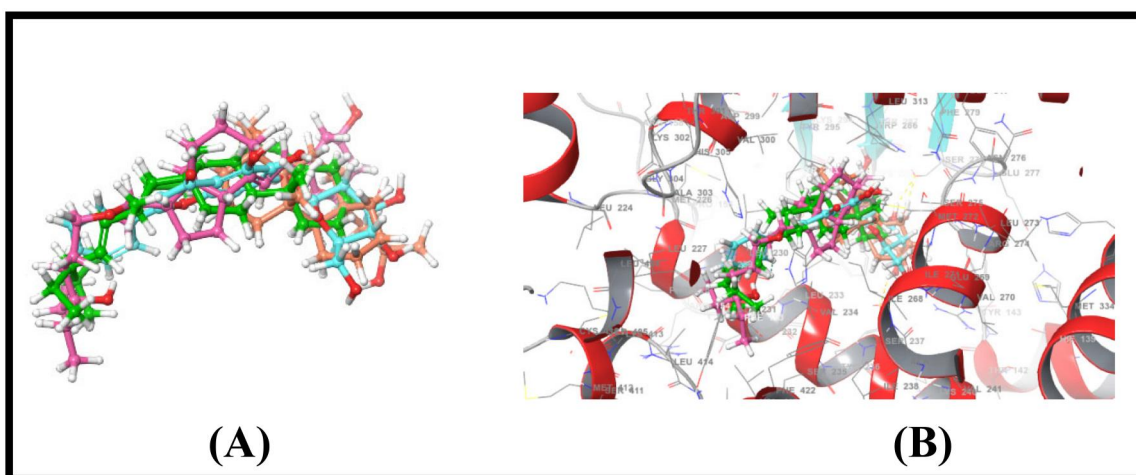
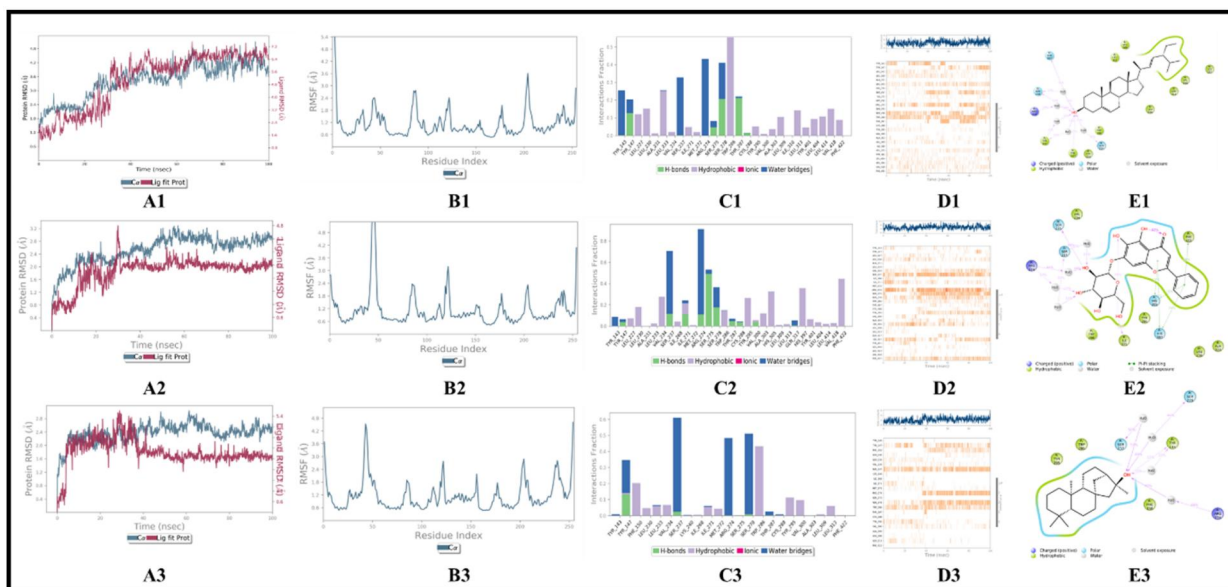


Figure 6. Superimposition of co-crystallized ligand and the best docked pose of stigmaterol, baicalein-7-o-glucoside, and kauran-16-ol (A), at the active pocket of VDR is depicted in Figure 6B, which reveals that stigmaterol and KH1060 share a common binding pattern.



**Figure 7.** RMSD plot of the protein–ligand complex (PDB ID: 1LPB) (A1, A2, A3), RMSF plot (B1, B2, B3), stacked bar plot of the fraction of time of the interactions (C1, C2, C3), Protein–ligand contacts (D1, D2, D3) and Ligand–Protein contacts (E1, E2, E3) of stigmasterol, baicalein-7-o-glucoside, kauran-16-ol for 100 ns of simulation time, respectively.

**Residue mobility analysis:** The Root Mean Square Fluctuation (RMSF) typically represents the N and C- terminals of the amino acids which are responsible for additional fluctuation as compared to the rest part of the protein. Alpha helices and beta strands are comparatively more stable than their unstructured portion. Here, the residue-wise fluctuations of the ligand–protein complexes are determined for the entire 100 ns simulation time. From the stigmasterol–VDR complex, the region of amino acid residues 10–190 is having the RMSF of  $<3.0\text{Å}$ , indicating the non-fitness of Stigmasterol into the binding pocket of the VDR receptor, which correlates with the results obtained from stability analysis. From the baicalein 7-O-glucoside–VDR complex, throughout the amino acid residues only except residue 50, the RMSF is  $<3.0\text{Å}$ . From (-)-kauran-16-ol–VDR complex, the region of amino acid residues 50–240 is having the RMSF of  $<3.0\text{Å}$ .

**Protein–ligands contact analysis:** By monitoring the interaction pattern of VDR and Stigmasterol throughout the 100 ns simulation time, the protein–ligand contacts can be predicted. On a holistic note, the protein–ligand interaction can be divided into four classes, viz, ionic interactions, H-bond and hydrophobic interactions, and water bridges that can be visualized *via* the ‘Simulation Interactions Diagram’ panel. The 0.5 value of the Y-axis of the stacked bar plot suggests that 50% of the simulation time the specific interaction is maintained.

From the bar diagram, it can be seen that  $>50\%$  of the residues are responsible for the hydrophobic contacts with stigmasterol. The rest 50% are either responsible for the H-bond interactions or water bridges. None of the amino acid residues are responsible for ionic contacts. Trp 286 residue is solely responsible for the highest hydrophobic contact at  $>0.5$  interaction fraction. Tyr 143, Ser 237, and Arg 274 residues are solely responsible for the maximum water bridging interactions at around 0.2, 0.3, and 0.4 interaction

fractions, respectively. However, Tyr 147, Ser 275, Ser 278, and Thr 287 residues are responsible for forming both H-bonds and water bridges.

From the bar diagram, it can be seen that almost 50% of the residues are responsible for the hydrophobic contacts with baicalein 7-O-glucoside. Among the H-bond forming residues, Ser 275 residue is highly responsible for the H-bond formation at 0.4 interaction fraction. Ser 237 and Arg 275 residues are responsible for the highest water bridging at 0.6 and 0.8 interaction fractions, respectively.

From the bar diagram, it can be seen that most of the amino acid residues are responsible for either hydrophobic contacts or water bridges with (-)-kauran-16-ol. H-bond forming residues (Tyr 147, Ser 237, and Ser 278) are almost negligible. Phe 150 and Trp 286 are responsible for maximum hydrophobic contacts at 0.2 and 0.4 interaction fractions, respectively. Tyr 147, Ser 237, Arg 274, and Ser278 are responsible for the highest water bridging at 0.3, 0.6, 0.4, and 0.5 interaction fractions, respectively.

**3. In silico ADME/T studies:** The best three binding energy-containing compounds [Stigmasterol, baicalein-7-o-glucoside, and (-)-kauran-16-ol] were evaluated for their *in silico* pharmacokinetic and physicochemical parameters. From the SwissADME-generated data, all the properties were tabulated in the Table S7. From SwissADME-predicted data, it could be seen that the phytoconstituents showed significant values for the properties analyzed and on the basis of physicochemical properties, they exhibited drug-like characteristics. Stigmasterol and (-)-kauran-16-ol both obeyed Veber’s rule filter, while baicalein-7-o-glucoside obeyed Ghose’s rule. From the egg-boiled diagram, it was shown that only except kauran-16-ol, the other two phytoconstituents did not cross the blood brain barrier (BBB). Only baicalein-7-o-glucoside was found to be P-glycoprotein (P-gp) substrate, and is responsible for the efflux of the foreign particles out of the cells. All three phytoconstituents were not found to be the



inhibitors of most of the cytochrome P450 enzymes (CYP), while only (-)-kauran-16-ol was found to be the inhibitors of CYP1A2 and CYP2C9 subtypes. The egg boil diagram (Daina & Zoete, 2016) imported from the SwissADME, also satisfy that above result (Figure 8).

#### 4. Discussion

Network pharmacology helps to understand the interactions of the secondary phytoconstituents from the traditional medicines with their respective targets and probably modulated pathways (Chandran et al., 2017). Also, previously multiple investigations have been made to trace the efficacy of the numerous secondary phytoconstituents to tackle multiple infectious (Khanal et al., 2021; 2021; Khanal & Patil, 2022) and non-infectious conditions (Duyu et al., 2021; Khanal & Patil, 2021; 2022) by implementing a series of network pharmacology tools. Similarly, in the present study, the network pharmacology approach was used to assess the probable interaction of the secondary phytoconstituents from *E. fluctuans* with multiple proteins; identified the chief action over the VDR protein.

The increased nitrogen metabolites due to the protein degradation are one of the cause in the pathogenesis of urolithiasis in our body. In this regard in the present study, we identified multiple pathways concerned with nitrogen metabolism. Also, we traced the numerous phytoconstituents components which are also reported for nitrogen homeostasis. Previously, p53 has been reported for the regulation of ammonia metabolism via the urea cycle to control polyamine biosynthesis (Li et al., 2019). In the present study, we identified the regulation of the p53 signaling pathway by triggering *MDM2*, *CCND2*, *CASP8*, and *CHEK1* reflecting its involvement in ameliorating nitrogen homeostasis. Also, activation of the ROS/NF- $\kappa$ B/MMP-9 pathway has been reported in the calcium-

induced kidney crystal deposition (Wu et al., 2021). In the present study, we identified the regulation of the NF-kappa B signaling pathway (KEGG entry: *hsa04064*) via the modulation of 4 genes namely *TNFRSF1A*, *CD14*, *PLAU*, and *CCL4*; suggests the amelioration of calcium associated kidney disease. Previously, the Rap1 signal ameliorates renal tubular injury (Xiao et al., 2014); herein, the phytoconstituents from *E. fluctuans* were traced to regulate the genes associated with Rap1 signaling pathways via the regulation of 5 genes namely *CTNBN1*, *RAP1A*, *ID1*, *RHOA*, and *PRKCA*; may trigger in the amelioration of urolithiasis.

In KEGG analysis, the results revealed that the majority of the regulated proteins by the bioactives were also involved in the Fluid shear stress and atherosclerosis. It was reported that the changes in urinary fluid shear stress may result in the aggregation of renal tubules which initiate the inflammation (Miravète et al., 2011). Further, some research findings revealed that there is high risk of nephrolithiasis in the patients having atherosclerosis (Hsu et al., 2016; Huang et al., 2020). The different genes expressed in fluid shear and atherosclerosis were also involved in the pathogenesis of nephrolithiasis and the inflammation due to the kidney stones. A previous study revealed that tumour necrosis factor (TNF) binds with TNF receptor 1 (TNFRSF1A) and increases the adhesion of CaOx crystals with the luminal membrane of renal tubules. In our study, the expressions of TNFRSF1A gene was modulated in the fluid shear stress and atherosclerosis pathway which indicates that the TNF receptor signaling may be involved in the crystallization of CaOx (Mulay et al., 2017). Though the influence of matrix metalloproteinase (MMP2) in crystallization is not yet explored; however, matrix metalloproteinase destruct the cartilage through macrophages which may responsible for the kidney stone formation (Blom et al., 2007). CaOx crystals are known to bind with macrophages monocyte chemoattractant protein- 1

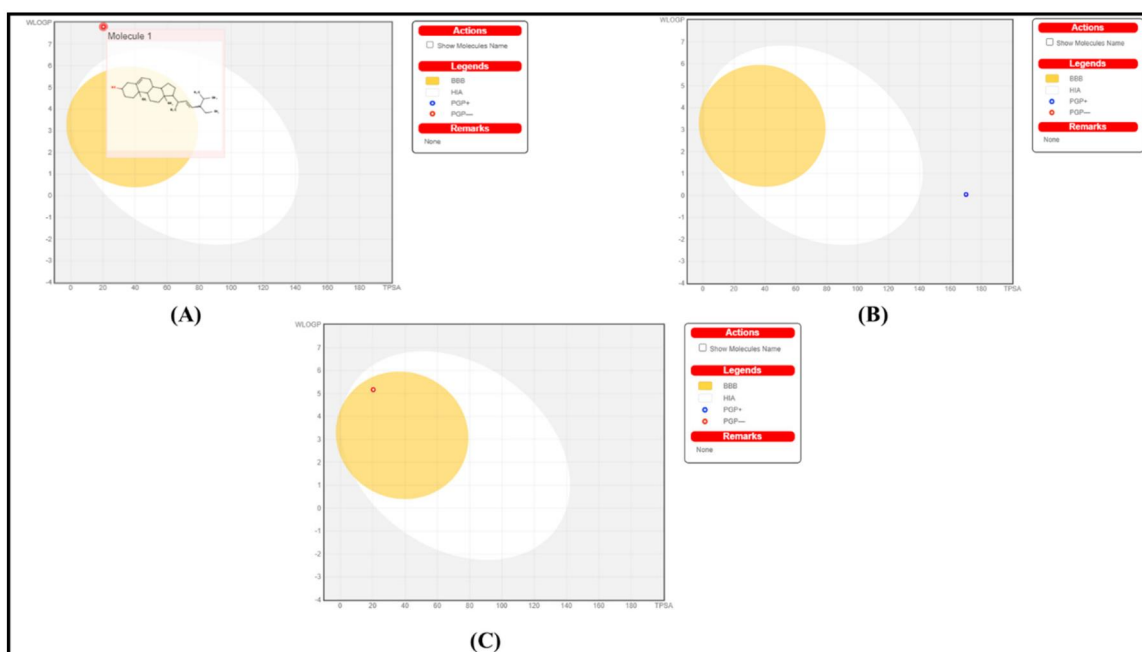


Figure 8. Egg boil diagram of stigmasterol (A), baicalein-7-o-glucoside (B), kauran-16-ol (C), imported from SwissADME.

(MCP-1) (also called as CCL2) to produce cytokines like TNF $\alpha$ , Interferon gamma or adhesive proteins like CTNNB1 also known as Catenin (cadherin-associated protein) beta 1 which aggregate the inflammation process during nephrolithiasis (de Water et al., 2001; Suen et al., 2010; Wigner et al., 2021). After exposure with CaOx crystals, the macrophages also secrete some factors which cause epithelial mesenchymal transition of renal tubular cells *via* RhoA-dependent TGF- $\beta$ 1 pathway (Kanlaya et al., 2013). The expression of nuclear factor (erythroid-derived 2)-like 2 (Nrf2, also called Nfe2l2) is also involved in inflammatory and oxidative stress pathways of nephrolithiasis (Zhu et al., 2019).

Molecular docking is an integral part of the system biology tool that helps to identify of the binding affinity of the lead molecules with their respective proteins (Khanal & Patil, 2022). Among all the phytoconstituents stigmasterol was found to have the highest Glide Score of  $-10.538$  kcal/mol and it shows the strong hydrophobic interaction in the binding site. The molecular simulations showed good protein-ligand stability. Also stigmasterol, baicalein-7-o-glucoside, and kauran-16-ol showed drug like properties in the *in silico* studies. Similarly, we traced the VDR as one of the majorly targeted proteins *via* the phytoconstituents included in the present study. Previously, activation of the VDR receptor has been reported in ameliorating kidney disease (Yang et al., 2018); hence, it can be reflected that activating this protein can contribute as a nephroprotective in urolithiasis as demonstrated in the present study.

Among the 25 different phytoconstituents,  $\alpha$ -pinene (Basar, 2014) and  $\beta$ -carotene (Holoch & Tracy, 2011) have been reported for their potential efficacy in relieving kidney stones. Previously, it has been reported that  $\alpha$ -pinene dissolves kidney stones (Basar, 2014). Similarly, in the present study, we identified  $\alpha$ -pinene to regulate six proteins and were also involved in modulating multiple pathways involved in nephrolithiasis. In addition, it has been pointed out that the  $\beta$ -carotene tends to prevent the formation of kidney stones (Holoch & Tracy, 2011). Likewise, we identified  $\beta$ -carotene to regulate the highest number of proteins (total count of 26) in the present work. This suggests that  $\beta$ -carotene from *E. fluctuans* may be playing an important role in the amelioration of nephrolithiasis.

In reporting to the limitation of the present work, this study did not examine the presence of each phytoconstituent experimentally which needs to be performed either *via* liquid chromatography-mass spectrum. In addition, the interactions of the phytoconstituents with predicted targets need to be further confirmed *via* the assessment of *in vivo* metabolic processes. Thus, this network pharmacology assessment of analysis of the *E. fluctuans* may include bias in the active compounds, targets, and pathways identification that is involved in the nephrolithiasis. Therefore, further functional studies need to be undertaken to validate the findings from this study.

## 5. Conclusion

Network pharmacology analysis elucidated the probable molecular mechanisms of *E. fluctuans* in managing nephrolithiasis; identified the lead molecules, their targets, and possible pathways. Results suggest that the VDR was found to be one of the majorly

targeted proteins *via* the included phytoconstituents in the study. In contrast, stigmasterol, baicalein-7-o-glucoside, kauran-16-ol were found to have a high affinity to bind with the VDR receptor confirmed by the molecular modelling and the dynamics. The VDR-baicalein-7-o-glucoside complex and VDR- kauran-16-ol complex showed better stability found in the *in silico* studies. Further, the experimental validation of the constructed network is still required to assess the interaction of the phytoconstituents with their respective targets to support the action of *E. fluctuans* over nephrolithiasis which is the future scope of present findings. The combination synergy network analysis based on the neighborhood approach can help us further to understand the mechanism of multi-molecular fixed-dose combinations.

## Acknowledgment

The authors are thankful to Science and Engineering Research Board (SERB), Department of Science and Technology, New Delhi for providing facilities for the research work (Project File number SRG/2021/001631).

## Consent to participate

All authors agree mutually with the participation in this work and declare that this is original research.

## Consent to publish

All authors read and approved the final manuscript for publication.

## Disclosure statement

The authors declare there are no conflicts of interest.

## Funding

This study is supported by Science and Engineering Research Board (SERB), Department of Science and Technology, New Delhi (Project File number SRG/2021/001631).

## Authors' contributions

YND: Conceptualization, Supervision, Formal Analysis, Writing (Review and Editing). BC, PK, AN, AD and AS: Data Collection, Investigation, Writing; SM: Revision.

## References

- Atanasov, A. G., Zotchev, S. B., Dirsch, V. M., & Supuran, C. T. (2021). International natural product sciences taskforce & supuran, C.T. natural products in drug discovery: advances and opportunities. *Nature Reviews Drug Discovery*, 20(3), 200–216. <https://doi.org/10.1038/s41573-020-00114-z>
- Auti, P. S., Nandi, A., Kumari, V., & Paul, A. T. (2022). Design, synthesis, biological evaluation and molecular modelling studies of oxoacetamide warhead containing indole-quinazolinone based novel hybrid analogues as potential pancreatic lipase inhibitors. *New Journal of Chemistry*, 46(24), 11648–11661. <https://doi.org/10.1039/D2NJ01210C>
- Barua, A., Alam, M. S., Junaid, M., Akter, Y., Afrose, S. S., Sharmin, T., Akter, R., & Hosen, S. M. Z. (2021). Phytochemistry, traditional uses and pharmacological properties of *Enhydra fluctuans* Lour: a Comprehensive Review. *Current Pharmaceutical Biotechnology*, 22(8), 1061–1068. <https://doi.org/10.2174/1389201021666200922161529>

- Başar, A. (2014). The dissolving effect of  $\alpha$ - and  $\beta$  pinenes in pine resin to kidney stone. *Journal of Medicinal Plants*, 2(6), 085–087. <https://doi.org/10.15413/ajmp.2014.0106>
- Blom, A. B., Van Lent, P. L., Libregts, S., Holthuysen, A. E., Van Der Kraan, P. M., Van Rooijen, N., & Van Den Berg, W. B. (2007). Crucial role of macrophages in matrix metalloproteinase-mediated cartilage destruction. *Arthritis and Rheumatism*, 56(1), 147–157. <https://doi.org/10.1002/art.22337>
- Chandran, U., Mehendale, N., Patil, S., Chaguturu, R., & Patwardhan, B. (2017). Network Pharmacology. *Innovative Approaches in Drug Discovery*, 127–164. <https://doi.org/10.1016/B978-0-12-801814-9.00005-2>
- Chattaraj, B., Nandi, A., Das, A., Sharma, A., Dey, Y. N., Kumar, D., & R, M. (2022). Inhibitory activity of *Enhydra fluctuans* Lour. on calcium oxalate crystallisation through *in silico* and *in vitro* studies. *Frontiers in Pharmacology*, 13, 982419. <https://doi.org/10.3389/fphar.2022.982419>
- Daina, A., & Zoete, V. (2016). A boiled-egg to predict gastrointestinal absorption and brain penetration of small molecules. *ChemMedChem*, 11(11), 1117–1121. <https://doi.org/10.1002/cmdc.201600182>
- Daina, A., Michielin, O., & Zoete, V. (2017). SwissADME: A free web tool to evaluate pharmacokinetics, drug-likeness and medicinal chemistry friendliness of small molecules. *Scientific Reports*, 7(1), 1–13. <https://doi.org/10.1038/srep42717>
- de Water, R., Leenen, P. J., Noordermeer, C., Nigg, A. L., Houtsmuller, A. B., Kok, D. J., & Schr, F. H. (2001). Cytokine production induced by binding and processing of calcium oxalate crystals in cultured macrophages. *American Journal of Kidney Diseases: The Official Journal of the National Kidney Foundation*, 38(2), 331–338. <https://www.sciencedirect.com/science/article/abs/pii/S0272638601689339>
- Duyu, T., Khanal, P., Dey, Y. N., & Jha, S. (2021). Network pharmacology of *Withania somnifera* against stress associated neurodegenerative diseases. *Advances in Traditional Medicine*, 21(3), 565–578. <https://doi.org/10.1007/s13596-020-00530-x>
- Friesner, R. A., Banks, J. L., Murphy, R. B., Halgren, T. A., Klicic, J. J., Mainz, D. T., Repasky, M. P., Knoll, E. H., Shelley, M., Perry, J. K., Shaw, D. E., Francis, P., & Shenkin, P. S. (2004). Glide: A new approach for rapid, accurate docking and scoring. 1. Method and assessment of docking accuracy. *Journal of Medicinal Chemistry*, 47(7), 1739–1749. <https://doi.org/10.1021/jm0306430>
- Ghelani, H., Chapala, M., & Jadav, P. (2016). Diuretic and antirolithiatic activities of an ethanolic extract of *Acorus calamus* L. rhizome in experimental animal models. *Journal of Traditional and Complementary Medicine*, 6(4), 431–436. <https://doi.org/10.1016/j.jtcme.2015.12.004>
- Holoch, P. A., & Tracy, C. R. (2011). Antioxidants and self-reported history of kidney stones: the National Health and Nutrition Examination Survey. *Journal of Endourology*, 25(12), 1903–1908. <https://doi.org/10.1089/end.2011.0130>
- Hsu, C. Y., Chen, Y. T., Huang, P. H., Leu, H. B., Su, Y. W., Chiang, C. H., Chen, J. W., Chen, T. J., Lin, S. J., & Chan, W. L. (2016). The association between urinary calculi and increased risk of future cardiovascular events: A nationwide population-based study. *Journal of Cardiology*, 67(5), 463–470. <https://www.sciencedirect.com/science/article/pii/S0914508715002294> <https://doi.org/10.1016/j.jcc.2015.07.016>
- Huang, H. S., Liao, P. C., & Liu, C. J. (2020). Calcium kidney stones are associated with increased risk of carotid atherosclerosis: The link between urinary stone risks, carotid intima-media thickness, and oxidative stress markers. *Journal of Clinical Medicine*, 9(3), 729. <https://doi.org/10.3390/jcm9030729>
- Kanehisa, M., Sato, Y., Kawashima, M., Furumichi, M., & Tanabe, M. (2016). KEGG as a reference resource for gene and protein annotation. *Nucleic Acids Research*, 44(D1), D457–D462. <https://doi.org/10.1093/nar/gkv1070>
- Kanlaya, R., Sintiprungrat, K., & Thongboonkerd, V. (2013). Secreted products of macrophages exposed to calcium oxalate crystals induce epithelial mesenchymal transition of renal tubular cells via RhoA-dependent TGF- $\beta$ 1 pathway. *Cell Biochemistry and Biophysics*, 67(3), 1207–1215. <https://doi.org/10.1007/s12013-013-9639-z>
- Khanal, P., & Patil, B. M. (2021). Consolidation of network and experimental pharmacology to divulge the antidiabetic action of *Ficus benghalensis* L. bark. 3 *Biotech*, 11(5), 238. <https://doi.org/10.1007/s13205-021-02788-7>
- Khanal, P., & Patil, B. M. (2022). Reversal of insulin resistance by *Ficus benghalensis* bark in fructose-induced insulin-resistant rats. *Journal of Ethnopharmacology*, 284, 114761. <https://doi.org/10.1016/j.jep.2021.114761>
- Khanal, P., Duyu, T., Patil, B. M., Dey, Y. N., Pasha, I., Kavalapure, R. S., Chand, S., & Gurav, S. (2021). Screening of JAK-STAT modulators from the antiviral plants of Indian traditional system of medicine with the potential to inhibit 2019 novel coronavirus using network pharmacology. 3 *Biotech*, 11(3), 119. <https://doi.org/10.1007/s13205-021-02664-4>
- Khanal, P., Patil, B. M., Mandar, B. K., Dey, Y. N., & Duyu, T. (2019). Network pharmacology-based assessment to elucidate the molecular mechanism of anti-diabetic action of *Tinospora cordifolia*. *Clinical Phytoscience*, 5(1), 35. <https://doi.org/10.1186/s40816-019-0131-1>
- Khanal, P., Zargari, F., Far, B. F., Kumar, D., Mogana, R., Mahdi, Y. K., Jubair, N. K., Saraf, S. K., Bansal, P., Singh, R., Selvaraja, M., & Dey, Y. N. (2021). Integration of system biology tools to investigate huperzine A as an anti-alzheimer agent. *Frontiers in Pharmacology*, 12, 785964. <https://doi.org/10.3389/fphar.2021.785964>
- Kuri, S., Billah, M. M., Rana, S. M., Naim, Z., Islam, M. M., Hasanuzzaman, M., Ali, M. R., & Banik, R. (2014). Phytochemical and *in vitro* biological investigations of methanolic extracts of *Enhydra fluctuans* Lour. *Asian Pacific Journal of Tropical Biomedicine*, 4(4), 299–305. <https://doi.org/10.12980/APJTB.4.2014C677>
- Lagunin, A., Ivanov, S., Rudik, A., Filimonov, D., & Poroikov, V. (2013). DIGEP-Pred: Web service for *in silico* prediction of drug-induced gene expression profiles based on structural formula. *Bioinformatics*, 29(16), 2062–2063. <https://doi.org/10.1093/bioinformatics/btt322>
- Li, L., Mao, Y., Zhao, L., Li, L., Wu, J., Zhao, M., Du, W., Yu, L., & Jiang, P. (2019). p53 Regulation of ammonia metabolism through urea cycle controls polyamine biosynthesis. *Nature*, 567(7747), 253–256. <https://doi.org/10.1038/s41586-019-0996-7>
- Miravète, M., Klein, J., Besse-Patin, A., Gonzalez, J., Pecher, C., Bascands, J. L., Mercier-Bonin, M., Schanstra, J. P., & Buffin-Meyer, B. (2011). Renal tubular fluid shear stress promotes endothelial cell activation. *Biochemical and Biophysical Research Communications*, 407(4), 813–817. <https://www.sciencedirect.com/science/article/abs/pii/S0006291X1100516X>
- Mulay, S. R., Eberhard, J. N., Desai, J., Marschner, J. A., Kumar, S. V., Weidenbusch, M., Grigorescu, M., Lech, M., Eltrich, N., Müller, L., Hans, W., Hrabě de Angelis, M., Vielhauer, V., Hoppe, B., Asplin, J., Burzlaff, N., Herrmann, M., Evan, A., & Anders, H. J. (2017). Hyperoxaluria requires TNF receptors to initiate crystal adhesion and kidney stone disease. *Journal of the American Society of Nephrology*, 28(3), 761–768. <https://jasn.asnjournals.org/content/28/3/761.short> <https://doi.org/10.1681/ASN.2016040486>
- Nandi, A., Das, A., Dey, Y. N., & Roy, K. (2023). The Abundant Phytocannabinoids in Rheumatoid Arthritis: Therapeutic Targets and Molecular Processes Identified Using Integrated Bioinformatics and Network Pharmacology. *Life*, 13(3), 700. <https://doi.org/10.3390/life13030700>
- Pak, C. Y. (1989). Prevention and treatment of kidney stones. Role of medical prevention. *Journal of Urology*, 141(3 Part 2), 798–801. [https://doi.org/10.1016/S0022-5347\(17\)41013-5](https://doi.org/10.1016/S0022-5347(17)41013-5)
- Rahman, M. (2019). Karyomorphological study of *Enhydra fluctuans* Lour. (Asteraceae). *Bangladesh Journal of Scientific and Industrial Research*, 54(4), 283–288. <https://doi.org/10.3329/bjsir.v54i4.44562>
- Sastry, M., Adzhigirey, G. M., Day, T., Annabhimoju, R., & Sherman, W. (2013). Protein and ligand preparation: parameters, protocols, and influence on virtual screening enrichments. *Journal of Computer-Aided Molecular Design*, 27(3), 221–234. <https://doi.org/10.1007/s10822-013-9644-8>
- Schrödinger Release 2017-2: Desmond Molecular Dynamics System, D. E. Shaw Research, New York, NY, 2017. Maestro-Desmond Interoperability Tools, Schrödinger, New York, NY, 2017.
- Schrödinger Release 2017-2: Glide. (2017). Schrödinger, LLC.
- Schrödinger Release 2017-2: LigPrep. (2017). Schrödinger, LLC.
- Schrödinger Release 2017-2: Protein Preparation Wizard; Epik, Schrödinger, LLC, New York, NY, 2017; Impact, Schrödinger, LLC, New York, NY; Prime, Schrödinger, LLC, New York, NY, 2017.

- Schrödinger Release 2017-2: QikProp. (2017). Schrödinger, LLC.
- Shannon, P., Markiel, A., Ozier, O., Baliga, N. S., Wang, J. T., Ramage, D., Amin, N., Schwikowski, B., & Ideker, T. (2003). Cytoscape: A software environment for integrated models of biomolecular interaction networks. *Genome Research*, 13(11), 2498–2504. <https://doi.org/10.1101/gr.1239303>
- Sharma, D., Dey, Y. N., Sikarwar, I., Sijoria, R., Wanjari, M. M., & Jadhav, A. D. (2016). *In vitro* study of aqueous leaf extract of *Chenopodium album* for inhibition of calcium oxalate and brushite crystallization. *Egyptian Journal of Basic and Applied Sciences*, 3(2), 164–171. <https://doi.org/10.1016/j.ejbas.2016.02.001>
- Sikarwar, I., Dey, Y. N., Wanjari, M. M., Sharma, A., Gaidhani, S. N., & Jadhav, A. D. (2017). *Chenopodium album* Linn. leaves prevent ethylene glycol-induced urolithiasis in rats. *Journal of Ethnopharmacology*, 195, 275–282. <https://doi.org/10.1016/j.jep.2016.11.031>
- Suen, J. L., Liu, C. C., Lin, Y. S., Tsai, Y. F., Juo, S. H., & Chou, Y. H. (2010). Urinary chemokines/cytokines are elevated in patients with urolithiasis. *Urological Research*, 38(2), 81–87. <https://doi.org/10.1007/s00240-010-0260-y>
- Swapana, N., Singh, C., & B, S. (2011). Herbal folk medicines used for urinary and calculi/stone cases complaints in Manipur, *NeBIO*, 2, 1–5.
- Szklarczyk, D., Gable, A. L., Lyon, D., Junge, A., Wyder, S., Huerta-Cepas, J., Simonovic, M., Doncheva, N. T., Morris, J. H., Bork, P., Jensen, L. J., & Mering, C. V. (2019). STRING v11: Protein–protein association networks with increased coverage, supporting functional discovery in genome-wide experimental datasets. *Nucleic Acids Research*, 47(D1), D607–D613. <https://doi.org/10.1093/nar/gky1131>
- Wigner, P., Grębowski, R., Bijak, M., Szemraj, J., & Saluk-Bijak, J. (2021). The molecular aspect of nephrolithiasis development. *Cells*, 10(8), 1926. <https://doi.org/10.3390/cells10081926>
- Wu, Y., Zhang, J., Li, C., Hu, H., Qin, B., Wang, T., Lu, Y., & Wang, S. (2021). The activation of ROS/NF-κB/MMP-9 pathway promotes calcium-induced kidney crystal deposition. *Oxidative Medicine and Cellular Longevity*, 2021, e8836355. <https://doi.org/10.1155/2021/8836355>
- Xiao, L., Zhu, X., Yang, S., Liu, F., Zhou, Z., Zhan, M., Xie, P., Zhang, D., Li, J., Song, P., Kanwar, Y. S., & Sun, L. (2014). Rap1 ameliorates renal tubular injury in diabetic nephropathy. *Diabetes*, 63(4), 1366–1380. <https://doi.org/10.2337/db13-1412>
- Yang, S., Li, A., Wang, J., Liu, J., Han, Y., Zhang, W., Li, Y. C., & Zhang, H. (2018). Vitamin D receptor: A novel therapeutic target for kidney diseases. *Current Medicinal Chemistry*, 25(27), 3256–3271. <https://doi.org/10.2174/0929867325666180214122352>
- Zhu, J., Wang, Q., Li, C., Lu, Y., Hu, H., Qin, B., Xun, Y., Zhu, Y., Wu, Y., Zhang, J., & Wang, S. (2019). Inhibiting inflammation and modulating oxidative stress in oxalate-induced nephrolithiasis with the Nrf2 activator dimethyl fumarate. *Free Radical Biology and Medicine*, 134, 9–22. <https://www.sciencedirect.com/science/article/pii/S0891584918315739> <https://doi.org/10.1016/j.freeradbiomed.2018.12.033>